THE STRONG COUPLING LIMIT OF SU(2) QCD AT FINITE BARYON DENSITY

E. DAGOTTO, F. KARSCH and A. MOREO

Department of Physics, University of Illinois at Urbana-Champaign, 1110 West Green Street, Urbana, IL 61801, USA

Received 24 January 1986

The thermodynamics is studied of SU(2) gauge theory with staggered fermions at finite baryon density and zero temperature in the strong coupling limit. Monte Carlo simulation and mean field analysis give a consistent picture indicating that no chiral phase transition occurs at $g^2 = \infty$ although the mesonic condensate $\langle \bar{\psi}\psi \rangle$ turns out to vanish for all non-zero chemical potentials.

Recently much effort has been put into the analysis of the phase structure of QCD with dynamical fermions. While these calculations gave convincing evidence for a chiral symmetry restoring phase transition at finite temperature [‡1], still very little is known about the influence of a finite chemical potential on the thermodynamics. This is partly due to the fact that in the presence of a non-vanishing chemical potential μ the euclidean action for SU(3), i.e. the fermion determinant, becomes complex [2] and thus standard Monte Carlo (MC) techniques cannot be applied [3]. MC simulations for QCD at finite baryon density have therefore only been performed in the quenched approximation [2] or using the color group SU(2) where the action is still real [4].

In addition there have been some attempts to analyze the phase structure of SU(N) gauge theories at finite density in the strong coupling limit using analytic techniques [5,6] like a $1/d$ expansion combined with a mean field (MF) analysis [7]. These calculations suggest the existence of a first-order chiral transition for SU(3) and a second-order transition for SU(2) in the strong coupling, $g^2 = \infty$, zero temperature, $T = 0$, limit. However, in attempting to compare these MF results with MC simulations performed for the SU(2) gauge theory with dynamical fermions in the same limit we could not find agreement between both approaches. This is rather astonishing as it is well known that results obtained at $g^2 = \infty$ from $1/d$ and MF calculations at $\mu = 0$, $T = 0$ agree quite well with MC results even on a quantitative level [7,8]. We thus expected that the MF ansatz used in refs. [5,6] might be too crude and decided to develop a more refined $1/d$, mean field analysis which handles the mesonic and baryonic sector of the effective action more carefully and also takes into account the spacetime asymmetry introduced by a non-vanishing chemical potential by allowing the fields to take on different mean values in space and time directions. This approach turns out to give results in good agreement with the MC data. Both approaches indicate that at $g^2 = \infty$, $T = 0$, $\mu \neq 0$ there is no chiral symmetry restoring transition. Nonetheless the mesonic condensate $\langle \bar{\psi}\psi \rangle$ turns out to vanish for all non-zero chemical potentials in the limit $m \to 0$. It turns out that the breaking of chiral symmetry is then due to non-vanishing baryonic condensates.

In the following we will present our MF approach for the SU(2) theory and compare the results with those obtained from a MC simulation where dynamical fermions have been incorporated using the pseudofermion algorithm [9]. At $g^2 = \infty$ the SU(2) partition function with non-vanishing chemical potential, $\mu \neq 0$, is given by

[‡1] For a recent review see ref. [1].

$$Z = \int \prod_x \mathrm{d}\chi_x \, \mathrm{d}\bar{\chi}_x \prod_{x,\mu} \mathrm{d}U_{x,\mu} \exp(-S_\mathrm{F}) , \tag{1}$$

with the fermion action, S_F, for staggered fermions given by

$$S_\mathrm{F} = \sum_x \Big(ma\bar{\chi}_x\chi_x + \tfrac{1}{2}\sum_{i=1}^{d} \eta_i(x)\bar{\chi}_x [U_{x,i}\chi_{x+i} - U^\dagger_{x-i,i}\chi_{x-i}] + \tfrac{1}{2}\bar{\chi}_x [\exp(\mu a) U_{x,0}\chi_{x+0} - \exp(-\mu a) U^\dagger_{x-0,0}\chi_{x-0}] \Big) , \tag{2}$$

where d denotes the space dimensions, a is the lattice spacing, m is the fermion mass and the phase factors $\eta_i(x)$ are defined as $\eta_i(x) = (-1)^{x_0+\ldots+x_{i-1}}$. In eqs. (1), (2) we have suppressed the color indices. The rest of the notation is the standard one.

In the $g^2 = \infty$ limit the integrals over the gauge fields $U_{x,\mu}$ are decoupled and can be performed exactly. This leads to the partition function

$$Z = \int \prod_x \mathrm{d}\chi_x \, \mathrm{d}\bar{\chi}_x \exp(-S_\mathrm{eff}) , \tag{3a}$$

with the effective action S_eff given by

$$S_\mathrm{eff} = \sum_x \Big(ma \sum_{a=1}^{2} \bar{\chi}^a_x\chi^a_x - \tfrac{1}{8}\sum_{\mu=0}^{d}\sum_{a,b=1}^{2} \bar{\chi}^a_x\chi^a_x\bar{\chi}^b_{x+\mu}\chi^b_{x+\mu} - \tfrac{1}{2}\sum_{i=1}^{d} (\det A_{x,i} + \det \bar{A}_{x,i})$$

$$- \tfrac{1}{2}[\exp(2\mu a)\det A_{x,0} + \exp(-2\mu a)\det \bar{A}_{x,0}] + \tfrac{1}{8}\sum_{\mu=0}^{d} \det A_{x,\mu} \det \bar{A}_{x,\mu} \Big) , \tag{3b}$$

and

$$\det A_{x,\mu} = -\tfrac{1}{2}\bar{\chi}^1_x\bar{\chi}^2_x\chi^1_{x+\mu}\chi^2_{x+\mu}, \quad \det \bar{A}_{x,\mu} = -\tfrac{1}{2}\chi^1_x\chi^2_x\bar{\chi}^1_{x+\mu}\bar{\chi}^2_{x+\mu}. \tag{4}$$

The action is now written in terms of composite meson–meson or baryon–antibaryon terms. In order to perform the integration over the Grassmann fields we have to split the four- and eight-fermion terms into bilinears of the fields, χ, $\bar{\chi}$. We do this by introducing auxiliary complex scalar fields $\sigma^\alpha_{x,\mu}$ which are defined on links x, μ of the lattice. Here $\alpha = 1, \ldots, 4$ labels the different fields necessary to decouple the different contributions to the effective action. The field $\sigma^1_{x,\mu}$ decouples the meson–meson interaction in eq. (3b) while $\sigma^2_{x,\mu}$ ($\sigma^3_{x,\mu}$) decouples $\det A_{x,\mu}$ ($\det \bar{A}_{x,\mu}$). Finally $\sigma^4_{x,\mu}$ is used to split the product of $\det A_{x,\mu}$ and $\det \bar{A}_{x,\mu}$ in the last term of eq. (3b). Thus for instance the baryon–antibaryon term in the effective action can be written as

$$\exp[\tfrac{1}{2}\exp(2\mu a)\det A_{x,0}] = \int\!\!\int_{-\infty}^{\infty} \frac{\mathrm{d}\,\mathrm{Re}\,\sigma^2_{x,0}\,\mathrm{d}\,\mathrm{Im}\,\sigma^2_{x,0}}{2\pi}$$

$$\times \exp\{-\tfrac{1}{2}\sigma^2_{x,0}\bar{\sigma}^2_{x,0} + [\exp(\mu a)/2\sqrt{2}](\sigma^2_{x,0}\bar{\chi}^1_x\bar{\chi}^2_x - \bar{\sigma}^2_{x,0}\chi^1_{x+0}\chi^2_{x+0})\}. \tag{5}$$

Note that this bosonoization has local character, i.e. it is valid in each link of the lattice. Similar formulas hold for the remaining terms in the action. A detailed description of this bosonization procedure [‡2] and a comparison with other approaches [5,6] will be given elsewhere [11]. As a result of this bosonization we obtain an effective action in terms of four scalar fields and the remaining bilinears of the Grassmann fields. These can now be inte-

[‡2] Similar bosonization tricks have been used in many different physical problems. For recent references see ref. [10].

grated out and we obtain the partition function in terms of scalar fields only

$$Z = \int \prod_{\alpha=1}^{4} \prod_{x,\mu} \mathrm{d}\sigma^{\alpha}_{x,\mu}\, \mathrm{d}\bar{\sigma}^{\alpha}_{x,\mu}\, \exp(-S_{\mathrm{eff}}), \tag{6}$$

with

$$S_{\mathrm{eff}} = \tfrac{1}{2} \sum_{x,\nu,\alpha} \sigma^{\alpha}_{x,\nu} \bar{\sigma}^{\alpha}_{x,\nu} - \sum_{x} \ln\Bigg[\Bigg(\sum_{\nu} \tfrac{1}{4}(\sigma^{1}_{x,\nu} + \bar{\sigma}^{1}_{x-\nu,\nu}) - ma\Bigg)^{2} + \tfrac{1}{8}\sum_{\nu} [(f^{+}_{\nu} + \tfrac{1}{2}\sigma^{4}_{x,\nu})^{1/2}\sigma^{2}_{x,\nu} + (f^{-}_{\nu} - \tfrac{1}{2}\bar{\sigma}^{4}_{x-\nu,\nu})^{1/2}\sigma^{3}_{x-\nu,\nu}]$$

$$\times \sum_{\lambda} [(f^{+}_{\lambda} + \tfrac{1}{2}\sigma^{4}_{x-\lambda,\lambda})^{1/2}\bar{\sigma}^{2}_{x-\lambda,\lambda} + (f^{-}_{\lambda} - \tfrac{1}{2}\sigma^{4}_{x,\lambda})^{1/2}\bar{\sigma}^{3}_{x,\lambda}]\Bigg], \tag{7a}$$

where

$$f^{\pm}_{\nu} = 1, \qquad \nu = 1, \ldots, d,$$
$$= \exp(\pm 2\mu a), \quad \nu = 0. \tag{7b}$$

Notice that eqs. (6), (7) are an exact rewriting of the original partition function eqs. (1), (2). Thus no approximations have been involved so far. We analyze the above partition function using a mean field ansatz for the different fields $\sigma^{\alpha}_{x,\mu}$ appearing in the action, eq. (7). As the action is rotational invariant in the d space dimensions we introduce identical mean fields in this directions, $\sigma^{\alpha}_{x,\mu} \to \sigma^{\alpha}$, $\mu \neq 0$, allow, however, a different mean value for the time like fields, $\sigma^{\alpha}_{x,0} \to \sigma^{\alpha}_{0}$. In this way we obtain as a mean field action

$$S^{\mathrm{MF}} = \tfrac{1}{2}\sum_{\alpha=1}^{4} (d\sigma^{\alpha 2} + \sigma^{\alpha 2}_{0}) - \ln([\tfrac{1}{2}(d\sigma^{1} + \sigma^{1}_{0}) - ma]^{2}$$

$$+ \tfrac{1}{8}\{(1 + \tfrac{1}{2}\sigma^{4})^{1/2}\sigma^{2}d + (1 - \tfrac{1}{2}\sigma^{4})^{1/2}\sigma^{3}d + [\exp(2\mu a) + \tfrac{1}{2}\sigma^{4}_{0}]^{1/2}\sigma^{2}_{0} + [\exp(-2\mu a) - \tfrac{1}{2}\sigma^{4}_{0}]^{1/2}\sigma^{3}_{0}\}^{2}). \tag{8}$$

Note that σ^{1}, σ^{1}_{0} are related to $\langle\bar{\chi}^{a}\chi^{a}\rangle$, i.e. the mesonic condensate, while σ^{2}, σ^{2}_{0}, σ^{3}, σ^{3}_{0} are related to $\langle\chi^{1}\chi^{2}\rangle$ or $\langle\bar{\chi}^{1}\bar{\chi}^{2}\rangle$ (baryonic condensates). Minimization of the mean field free energy, $F^{\mathrm{MF}} = S^{\mathrm{MF}}/V$, using standard numerical routines determines the saddle point in terms of the eight different scalar mean fields σ^{α}, σ^{α}_{0} which have been taken to be real. The mean field solution found this way, reflects the expected behavior of a fermion system at zero temperature but finite chemical potential, i.e. as long as the chemical potential, which at $T = 0$ defines the Fermi energy, is smaller than the energy of the lowest lying excited state above the vacuum, we are just probing the vacuum and all thermodynamic observables coincide with their $\mu = 0$ values. In the case of the SU(2) gauge theory this threshold value, μ_0, is determined by the lowest baryonic bound state which for SU(2) is degenerate with the lightest mesonic state. The threshold line $\mu_0(ma)$ (as well as the behavior of the mean field parameters) is shown in the phase diagrams, fig. 1. It separates the regime of vacuum physics (I) from the thermodynamic regime (II) and is given by [‡3]

$$\mu_0(ma) = \tfrac{1}{2}m_0(ma), \tag{9}$$

where m_0 is the energy of the lowest lying baryonic state [7]

$$m_0 = \ln[1 + \bar{d}(\bar{\lambda}^{2} - 1) + (2\bar{d}(\bar{\lambda}^{2} - 1) + \bar{d}^{2}(\bar{\lambda}^{2} - 1)^{2})^{1/2}], \tag{10}$$

[‡3] Although we could not prove eq. (9) analytically due to the large number of parameters involved in the minimization of F^{MF}, we checked that this relation holds to high numerical accuracy for all values of ma.

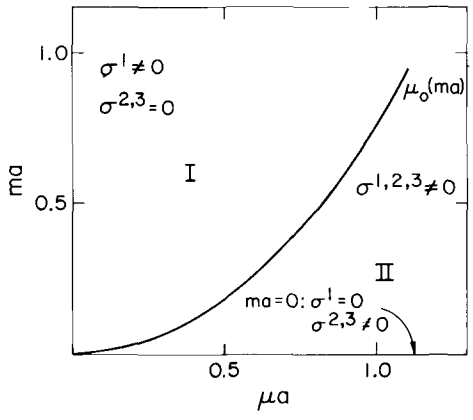

Fig. 1. The phase diagram of the $g^2 = \infty$, $T = 0$ SU(2) gauge theory with staggered fermions. The threshold line $\mu_0(ma)$ shown in the chemical potential (μa)–mass (ma) plane is given by eqs. (9), (10). It separates the vacuum regime (I) from the thermodynamic region (II). Also shown are the mean field values σ^α in the different regions.

$$\bar{\lambda} = ma/(2\bar{d})^{1/2} + [1 + (ma)^2/2\bar{d}]^{1/2}, \quad \bar{d} = d + 1. \qquad \text{(10 cont'd)}$$

Notice that in the μ–m phase diagram we do not observe any singular behavior of the mean field solutions in the whole thermodynamic regime (II).

Let us now discuss the behavior of some thermodynamic observables as a function of μ and m in more detail and compare the mean field results with those obtained from a Monte Carlo simulation. The Monte Carlo data have been obtained from simulations with dynamical fermions of mass $ma = 0.05, 0.1$ and 0.2 on a 4^4 lattice. In some cases we have checked that finite size effects are small in the $g^2 = \infty$ limit by performing simulations on a $8^3 \times 4$ lattice. Dynamical fermions have been simulated using a pseudofermion (PF) algorithm [9] with an acceptance rate of 90% and 250 iterations in the PF update to calculate the inverse fermion matrix [‡4]. The MC data shown are based on runs with 500 iterations at each value of ma and μa.

In fig. 2 we show the mesonic condensate $\langle\bar{\psi}\psi\rangle$ as a function of μa for various mass values, $ma = 0.05, 0.1$ and

‡4 For a discussion of the various approximations entering the pseudofermion update see e.g. ref. [12].

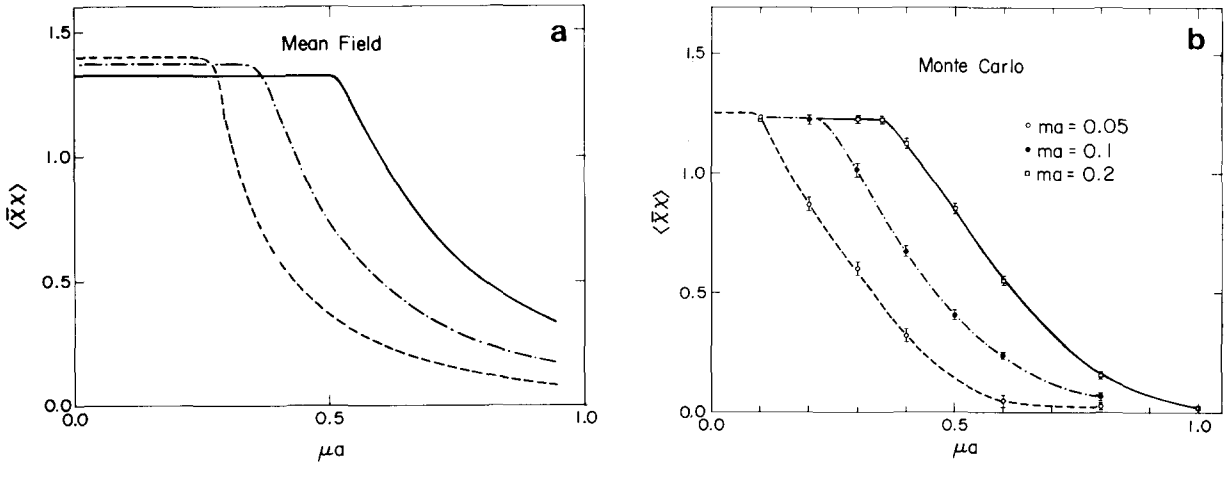

Fig. 2. The mesonic condensate $\langle\bar{\chi}\chi\rangle$ versus μa for three values of the fermion mass, $ma = 0.05$ (– –), 0.1 (– . –) and 0.2 (–). (a) shows the mean field results and (b) gives the Monte Carlo data. Lines are drawn in (b) to guide the eye.

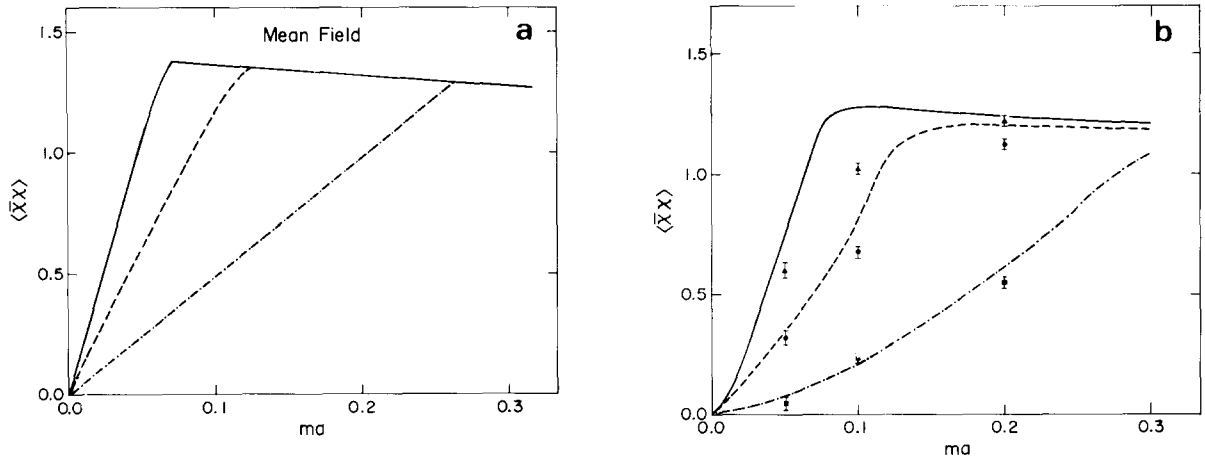

Fig. 3. The mesonic condensate $\langle\bar{\chi}\chi\rangle$ versus ma for three values of the chemical potential, $\mu a = 0.3$ (–), 0.4 (– –) and 0.6 (– . –). (a) shows the mean field results and (b) gives the Monte Carlo data obtained with a Lanczos algorithm [13] from 15 configurations generated with mass $ma = 0.1$ for each value of μa.

0.2. As can be seen $\langle\bar{\psi}\psi\rangle$ agrees with the $\mu a = 0$ result up to a threshold value which for the mean field calculations, fig. 2a, is just given by eqs. (9), (10). The MC data, fig. 2b, do not show the sharp cusp at $\mu_0(ma)$, which is probably due to finite size rounding effect. But they are clearly in good agreement with the mean field results. The behavior of $\langle\bar{\chi}\chi\rangle$ as a function of ma for some values of μa is shown in fig. 3. Again there is good agreement between the mean field, fig. 3a, and Monte Carlo, data shown in fig. 3b. The data points given in fig. 3b are obtained from averages over 300 iterations from our runs at $ma = 0.05$, 0.1 and 0.2 for the 3 values of $\mu a = 0.3$, 0.4 and 0.6. We also show the complete mass dependence of $\langle\bar{\chi}\chi\rangle$ obtained by applying the Lanczos algorithm [13] on 15 configurations (separated by 20 sweeps) of our runs at $ma = 0.1$. This stresses the similarity of the MC and MF results. It should, however, be noted that this procedure is rigorous only in the quenched approximation. Using the Lanczos approach to extrapolate to masses different from the one used in the unquenched MC simulations will introduce systematic errors. However, clearly these will not be visible within our limited statistics.

Obviously the results for $\langle\bar{\chi}\chi\rangle$ shown in fig. 3 indicate that

$$\lim_{ma\to 0} \langle\bar{\chi}\chi\rangle = 0 \quad \text{for all } \mu a > 0. \tag{11}$$

This somewhat unexpected result does, however, not mean that chiral symmetry is restored for all non-zero values of the chemical potential. In fact, we find that chiral symmetry remains broken for all $\mu > 0$. This is due to the creation of a baryonic condensate in the thermodynamic region (II) of the μ–m plane (see fig. 1).

$$B \equiv \langle \chi^1\chi^2 - \bar{\chi}^1\bar{\chi}^2\rangle = 0, \quad \mu(ma) \leqslant \mu_0(ma),$$
$$\neq 0, \quad \mu(ma) > \mu_0(ma). \tag{12}$$

The appearance of this condensate has been verified in the mean field calculations. To do so we have introduced a baryonic source in the action eq. (2), $S_J^{\mathrm{F}} = S^{\mathrm{F}} + J\Sigma_x(\chi_x^1\chi_x^2 - \bar{\chi}_x^1\bar{\chi}_x^2)$, and performed the mean field analysis for finite J. In the limit $J \to 0$ we recover our previous mean field solution and observe the spontaneous creation of the baryonic condensate $B = \mathrm{d}F/\mathrm{d}J|_{J=0}$. The behavior of this condensate is shown in fig. 4 for $ma = 0.0$ and 0.1. Clearly B is nonzero for $\mu > \mu_0(ma)$, i.e. for all $\mu > 0$ in the $ma = 0$ case. The baryonic condensate B breaks the

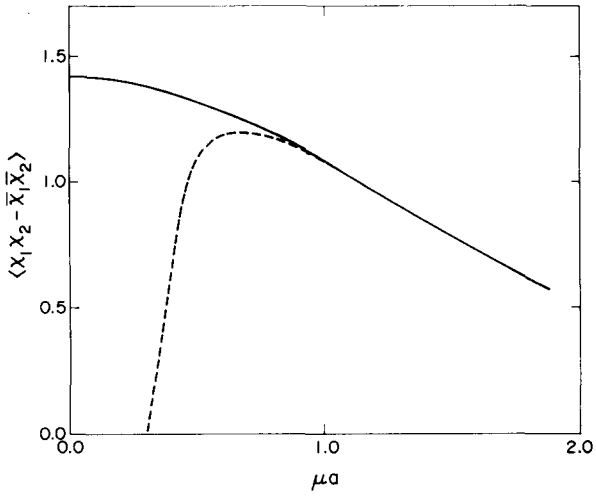

Fig. 4. The baryonic condensate $B = \langle \chi^1\chi^2 - \bar{\chi}^1\bar{\chi}^2 \rangle$ versus μa for $ma = 0.0$ (–) and 0.1 (– –) obtained from the mean field calculations.

$U_V(1)$ symmetry as well as the chiral symmetry of the massless fermion action. We thus conclude that chiral symmetry remains broken for all $\mu a \geqslant 0$ and no chiral symmetry restoring transition occurs in the SU(2) theory at $g^2 = \infty$, $T = 0$. This is also evident from the behavior of other thermodynamic observables, which will be discussed in detail elsewhere [11].

In general we find also that in the limit of large chemical potential all observables approach those of the free theory ($U_{x,\mu} \equiv 1$). However, it is also evident from fig. 3 that for all masses

$$\lim_{\mu a \to \infty} \langle \chi^1\chi^2 - \bar{\chi}^1\bar{\chi}^2 \rangle = 0, \tag{13}$$

and thus the chiral invariant, $U_V(1)$ symmetric limit of the free theory is only reached at infinite chemical potential. Notice also that in the case of SU(2) baryons are in fact bosons and indeed the condensate B is a Bose condensate. Thus one might speculate that this condensate disappears above some critical temperature $T_{ch}(\mu)$ which then would indicate a finite temperature chiral symmetry restoring transition. We are currently investigating this possibility.

The results presented here show a rather unexpected behavior of the strong coupling SU(2) theory at finite chemical potential in several respects. The mesonic condensate $\langle \bar{\chi}\chi \rangle$ turns out to be zero for $\mu a > 0$ and $ma = 0$. Nonetheless chiral symmetry as well as the $U_V(1)$ symmetry of the fermion action, eq. (2), is spontaneously broken due to a non-vanishing baryonic condensate $\langle \chi^1\chi^2 - \bar{\chi}^1\bar{\chi}^2 \rangle$. We would like to stress the fact that good agreement between MC and MF approach has mainly been achieved through the introduction of additional fields σ^2, σ^3 [eq. (8)] in the MF calculations. This accounts for the main difference compared with the MF results of refs. [4,5]. The appearance of a baryonic condensate has been observed up to now only in the MF calculations as our MC programs were not set up to deal with baryonic source terms. We plan, however, to analyze the baryon condensate in the future also in MC calculations.

Certainly it also deserves further study in how far the results presented here are specific to the SU(2) color group and the fact that baryons are bosons in this theory. To this extent we are presently investigating the strong coupling SU(3) theory with finite chemical potential. We hope that the MC analysis of this theory can be performed with a recently developed complex Langevin algorithm [3].

We thank I.M. Barbour and N.E. Behilil for providing us with a copy of their Lanczos programs and M. Stone, E. Fradkin, J. Verbaarschot and H.W. Wyld for many valuable discussions and helpful suggestions. This work was supported in part by the National Science Foundation grants PHY82-01948 and DMR84-15063.

References

[1] F. Karsch, QCD at finite temperature and baryon number density, Illinois preprint ILL-(TH)-86-#5 (January 1986).
[2] J. Kogut, H. Matsuoka, M. Stone, H.W. Wyld, S. Shenker, J. Shigemitsu and D.K. Sinclair, Nucl. Phys. B225 [FS9] (1983) 93.
[3] F. Karsch and H.W. Wyld, Phys. Rev. Lett. 55 (1985) 2242.
[4] A. Nakamura, Phys. Lett. 149B (1984) 391.
[5] P.H. Damgaard, D. Hochberg and N. Kawamoto, Phys. Lett. 158B (1985) 239.
[6] E.M. Ilgenfritz and J. Kripfganz, Z. Phys. C29 (1985) 79.
[7] See e.g. H. Kluberg-Stern, A. Morel and B. Petersson, Nucl. Phys. B215 [FS7] (1983) 527.
[8] E. Marinari, G. Parisi and C. Rebbi, Phys. Rev. Lett. 47 (1981) 1795.
[9] F. Fucito, E. Marinari, G. Parisi and C. Rebbi, Nucl. Phys. B180 [FS3] (1981) 369;
H.W. Hamber, E. Marinari, G. Parisi and C. Rebbi, Phys. Lett. 124B (1983) 99.
[10] U. Wolff, Nucl. Phys. B225 (1983) 391;
T. Eguchi and R. Nakayama, Phys. Lett. 126B (1983) 89.
[11] E. Dagotto, F. Karsch and A. Moreo, in preparation.
[12] R.V. Gavai and F. Karsch, Nucl. Phys. B261 (1985) 273.
[13] I.M. Barbour, J.P. Gilchrist, H. Schneider, G. Schierholz and M. Teper, Phys. Lett. 127B (1983) 433.